AGEING EFFECTS ON THE SMALL-STRAIN STIFFNESS OF A BIO-TREATED COMPACTED SOIL

Laura Morales[1], Enrique Romero[2*], Cristina Jommi[3], Eduardo Garzón[1] and Antonio Giménez[1]

Affiliation:

[1] Department of Engineering, Universidad de Almería, Carretera Sacramento s/n, Cañada de San Urbano, 04120 Almería, Spain, e-mail: mhl274@ual.es, egarzon@ual.es, agimfer@ual.es

[2] Department of Geotechnical Engineering and Geosciences, Universitat Politècnica de Catalunya, c/ Jordi Girona 1-3, Campus Nord UPC, Edificio D-2, 08014 Barcelona, Spain

[3] Department of Geoscience and Engineering, Faculty of Civil Engineering and Geosciences, Delft University of Technology, Stevinweg 1, 2628 CN Delft, The Netherlands, e-mail: c.jommi@tudelft.nl

*** Contact details:**

Prof. Enrique Romero
Departamento de Ingeniería del Terreno,
c/ Jordi Girona 1-3, Campus Nord, Edificio D-2
Universitat Politècnica de Catalunya,
08034 - Barcelona – Spain
Fax: +34-93 4017251
e-mail: enrique.romero-morales@upc.edu

Number of words in the main text: 2821
Number of tables: 2
Number of illustrations: 9

Abstract

The effect of ageing on the small-strain shear stiffness of compacted silty-clayey sand following a *soft* biological treatment is discussed. The samples were prepared by static compaction adding urea-degrading bacteria in the compaction water. No nutrients were artificially added, relying on the natural availability of urea and Ca^{2+} in the humic soil and in the compaction water for the bacteria to precipitate calcium carbonate. After compaction, part of the samples were cured in a system open to vapour transfer, and part of them in a closed system, to replicate different environmental boundary conditions. The small-strain shear stiffness was periodically tracked with bender elements during the ageing period. Tests were run in parallel to investigate the unconfined compression strength, the water retention properties and the soil pore size distribution changes during ageing. The tests results revealed a small but consistent increase in the small-strain shear stiffness during the ageing period due to the microbiological treatment, in both the closed and the open to vapour transfer systems. In the latter case, the contribution of the microbiological treatment to the increase in stiffness could be estimated after correcting the data for the suction increase due to evaporation.

Keywords: compacted soil, microbiological treatment, ageing, small-strain shear stiffness

Introduction

Sustainable development policies and environmental concerns in earthworks impel the research for new low carbon footprint construction techniques. To this aim, biological techniques are studied to improve the hydro-mechanical behaviour of soils naturally available on site and allow their use in earth structures (DeJong *et al.* 2013). A *soft* biological improvement for compacted earth construction in the South of Spain was recently discussed by Morales *et al*. (2015). The specific bio-treatment was conceived by the contractor to reduce the costs and the potential impact of produced ammonia to a minimum, at the same time ensuring proper performance of the compacted soil. The suggested methodology consisted in adding urea-degrading bacteria to a humic soil, in which the nutrients required for the precipitation of calcium carbonate are limited by the natural availability of Ca^{2+} and urea in the natural soil and in the compaction water (Hammes and Verstraete 2002; Al Qabany *et al*. 2012). To reproduce a likely field procedure, Bacillaceae microorganisms were added to the compaction water, and the samples were compacted after seven days curing. Morales *et al*. (2015) reported that this protocol induced the breakage of most bio-cemented bonds upon compaction, and that the slight mechanical improvement observed in the laboratory tests was mostly due to the fine fraction generated by broken bonds acting as a filler of the inter-grain porosity.

A modification to the original protocol is investigated here on the same humic silty-clayey sand, in an attempt to better preserve the bio-cement and improve the effectiveness of the bio-treatment. Static compaction was performed in this test series before microbiological ageing started.

The paper discusses the effects of ageing on the bio-treated soil, tracking its small-strain shear stiffness with bender elements, and looking at the results of some ancillary tests, namely unconfined compression strength and tensile splitting tests. Water retention data were collected to correct the information on soil stiffness for the effect of suction increase due to drying on the samples cured in the open environment. Mercury intrusion porosimetry tests, performed on selected samples at increasing curing periods, complement the experimental information on the effects of ageing at the microstructure scale.

Soil properties, bio-treatment and curing

The soil investigated is a humic silty-clayey sand from SE Spain, widely used in earthwork constructions (Morales *et al*. 2012, 2015), and a microorganism of the Bacillaceae family was used in the bio-treatment protocol (Morales *et al*. 2010, 2015). As schematically shown in Figure 1, a known concentration of bacteria previously isolated under laboratory conditions was inoculated into the natural and non-sterilised soil, together with a low-concentration saline solution (< 0.9%) to reach the optimum water content for compaction. No further nutrients were added, relying on natural availability of urea and Ca^{2+} in the soil and in the compaction water. Details of the procedure and availability requirements for urea and Ca^{+2}, are discussed in Morales *et al*. (2015). The main physical and chemical properties of the natural (untreated) and of the treated samples are summarised in Table 1.

As indicated in Figure 1, the samples were statically compacted before microbiological ageing (new protocol referred hereafter as ‘treated_NT’). The water content, dry density and degree of saturation of the natural material at optimum standard and modified

Proctor compaction are summarised in Table 2. Static compaction was chosen to match the optimum state reached with standard Proctor energy (0.6 MJ/m^3), and to better control the initial void ratio and degree of saturation. The maximum vertical stress and the initial suction corresponding to the static as-compacted state are included in the table.

After compaction, part of the samples were cured in a system open to vapour transfer ('open-system'), and part of them in a system closed to vapour transfer ('closed-system'), to provide ideal bounds for variable environmental conditions in the field. The results in Table 1 show that the calcium carbonate content systematically increased and reached 8.8% (Dietrich-Frühling method) after curing in this test series (NT). The chemical data show consistent changes in the soil properties due to the microorganism activity. The bacteria produced carbonates from hydrolysis of urea, and from the organic matter available in the soil, which decreased in the treated samples (reduction of 0.22% for test series NT that corresponds to a demand of 4.1 kg of organic matter per m^3 of compacted soil). Table 1 also shows that gypsum concentration in the soil decreased as a consequence of the alkaline pH of the bacterial environment (typically between 8.1 and 8.9), which leads to its dissolution and consequent release of Ca^{2+} cations (new source of Ca^{2+} supply for calcium carbonate precipitation).

Figure 1 shows the two different procedures followed after compaction for the ageing period, which lasted a minimum of seven days. In the 'open-system' procedure, characterised by O_2-rich conditions for microbial activity, cylindrical samples (either 38 mm in diameter and 76 mm high or 50 mm in diameter and 20 mm high) were placed in a desiccator and kept under a relative humidity higher than 97%. At specified intervals,

the samples were extracted from the vessels, weighed and tested, which induced some progressive evaporation. In this test series, the improvement of the mechanical properties could be due to both the bio-treatment and the suction increase due to drying. To distinguish between the two contributions, 'blank' tests were performed, by reproducing the same evaporation history on compacted samples of the original untreated soil. This blank series provided the reference for water content losses and soil stiffness changes due to suction increase during curing. The assumption was made that progressive drying affected both untreated and treated samples in the same way.

The 'closed-system' curing procedure was conceived to minimise evaporation effects. A smaller sample (50 mm in diameter and 20 mm high) was mounted in a closed oedometer cell, in which bender elements were allocated in the top and bottom caps. One sample was enough for multi-stage testing in this case: the oedometer was opened at specified intervals to quickly estimate the change in water content of the bio-treated material by measuring the mass loss. Both the desiccator and the oedometer cell were placed in an oven at 30°C to facilitate the growth of microorganisms during the incubation stage.

Water retention properties and pore size distribution: 'open-system' curing

A chilled mirror dew-point psychrometer (WP4, Decagon Devices) was used to measure total suction during multistage drying -from suctions greater than about 0.8 MPa up to 100 MPa- on compacted 'NT' samples after 7 days of ageing. Figure 2 presents the water retention data in terms of degree of saturation. Since the material did not experience significant shrinkage on suction increase, the drying curve corresponds to an approximately constant void ratio (e = 0.45÷0.47). Data on untreated and treated

samples using psychrometer readings and axis translation with volume change measurement from Morales *et al*. (2015) are also included. The three set of data do not differ substantially, which is consistent with the fact that the treatment hardly affects the specific surface of the soil (Table 1). Water retention results on drying are fitted to the model proposed by Romero *et al*. (2011), which is also plotted in the figure.

Mercury intrusion porosimetry tests were performed on freeze-dried samples at increasing 'open-system' curing periods. Tests were performed on natural and treated 'NT' samples after 2, 4 and 7 days of curing and at the same void ratio (e = 0.47). The cumulative distributions in terms of intruded void ratio and the corresponding pore size density functions of the different samples (PSD log differential intrusion) are reported in Figure 3. Maximum intruded void ratios were slightly below the as-compacted void ratio, indicated by the dashed horizontal line. The difference, which arises due to the non-intruded porosity for entrance pore sizes lower than 6 nm and the non-detectable porosity for pore sizes larger than 400 μm, increases with ageing. Test results indicate the development of bi-modal PSD functions, in which an entrance pore size around 5 μm was selected to separate the inter-grain (or inter-aggregate) pore sizes between grains and aggregates ('Macro' in the figure) from the intra-aggregate porosity inside the aggregates ('micro' in the figure). As indicated in the PSD plot, there are two pore size regions in which changes are hardly detected, namely the ranges 6-400 nm and 50-400 μm. The intra-aggregate (micro-) porosity (between 0.4 and 5 μm) tends to reduce systematically during ageing, with a corresponding increase of the inter-aggregate (macro-) porosity (between 5-50 μm), at almost constant void ratio. This is better shown in Figure 4, where the evolution of the macro-void ratio, e_M, and micro-void ratio, e_m, are plotted at different ageing periods ($e_m + e_M = e$). The reduction of the cumulative

micro-void ratio is in agreement with the decrease in water content due to evaporation (see legend of Figure 3) although, according to Romero (2013), for an average specific surface of 38 m^2/g (Table 1) the predicted decrease in e_m due to water content loss would be expected to be lower, around $\Delta e_m/\Delta w \approx -0.81$ (Figure 4). The difference between the prediction and the recorded data suggests that additional phenomena associated with the biological activity have to be considered. Possible mechanisms contributing to the reduction of the micro porosity can be identified with water consumption during hydrolysis of urea to CO_3^{2-} and ammonium cation (see, for instance, Stocks-Fischer *et al*. 1999), and occlusion of some micro-pore volume by calcified bacteria (vital size around 1 to 3 μm).

Mechanical tests: 'open-system' curing

Unconfined compression tests (ASTM D2166) and splitting tensile strength tests (ASTM C496) were conducted on untreated and 'NT' samples ∅ 38 mm × h 76 mm, and ∅ 50 mm × h 20 mm, respectively, to get preliminary information on the mechanical improvement. These destructive tests were run on independent samples that were cured under 'open-system' conditions before testing. Unconfined compression tests on 'NT' samples were performed at controlled displacement rate (0.3 mm/min) after 2, 4 and 7 days of ageing. The axial (deviatoric) stress - axial strain curves are plotted in Figure 5a. The data show an increase in the peak strength of the treated samples with ageing. The observation is confirmed by Figure 5b, in which splitting tensile strength results are also plotted. The maximum value for strength after 4 ageing days is a possible outlier, due to some additional drying that the sample underwent after curing and before testing.

To investigate in a more systematic way the preliminary results, and to correct for the suction increase due to drying, small-strain shear stiffness tests were performed on untreated (blank test) and treated 'NT' samples. A multi-stage procedure on a single sample was used to evaluate stiffness changes with bender elements. The small-strain shear modulus G along the vertical direction was tracked by measuring the shear wave velocity V_S, and calculated as $G = \rho V_S^2$, where ρ is the bulk density of the soil, and $V_S = l_{eff}/t_S$. The wave travel distance l_{eff} was taken as the distance between transducer tips, and the arrival time t_S was determined by inspection of the received trace, looking for the first significant amplitude excursion. A sine pulse V_{pp} = 20V with apparent input frequency 15 kHz was used as input signal. Additional details are given in Arroyo *et al*. (2010) and Pineda (2012).

A general increase in G with ageing is observed in the time evolution plot presented in Figure 6. Nevertheless, a decrease of the shear modulus is displayed between days 7 and 13, which is associated with the slight increase in the degree of saturation (from 70% to 72%) shown in Figure 7. The latter figure reports the evolution of the degree of saturation and total suction (measured with a psychrometer) at different curing times. The data highlight a higher drying rate during the first seven days, which slows down afterwards. The drying rate is mainly governed by evaporation during curing, but it is also partially affected by the amount of water required by the microorganisms to precipitate $CaCO_3$ minerals. The results of the blank test on the untreated sample, also reported in Figure 7, allow distinguishing the effects of evaporation form those of the microbiological treatment, and will be used in the following to correct the measured stiffness for suction.

The data in the Figures 4-7 suggest that the bio-treatment effects are non-linear with time, due to limiting factors on the microorganism activity. The most relevant are O_2 availability for microbial respiration (which reduces in 'closed-system' conditions), water availability for the hydrolysis of urea, and carbonates precipitation in soil pores which limit the vital space of microorganisms.

Bender element tests: 'closed-system' curing

The evolution of small-strain shear modulus during 'closed-system' curing, measured with a multi-stage procedure on a single sample, is reported in Figure 6. The variation in the degree of saturation of the sample is almost negligible in this case (between 87% and 85%), and it is due to the water mass required by the microbiological reactions. The 'closed-system' data are assumed to describe the stiffness increase induced only by the followed bio-treatment. The small-strain stiffness from a resonant column test performed at an isotropic confining of 0.1 MPa on an untreated sample by Morales *et al*. (2015) is presented for comparison.

Interpretation of the results

Figure 8a presents the evolution of the normalised values G/G_0 with the degree of saturation of both 'NT' and untreated samples in the 'open-system', by combining the information reported in Figures 6 and 7. In this and the following figures, G_0 indicates the small-strain shear stiffness of the untreated material before ageing. Figure 8b displays the evolution of the normalised values G/G_0 with time. Both samples underwent drying during curing in the 'open-system', and the small shear strain modulus increased as a consequence of suction increase. Nonetheless, the comparison

between the data also clearly shows the contribution of the bio-treatment to the small-strain stiffness increase with ageing.

The results of the blank test were modelled with the following expression for the small-strain shear stiffness under partially saturated states, which uses the constitutive stress $p' = p'' + S_r s$

$$\frac{G}{G_0} = \left(\frac{p'}{p'_0}\right)^{\alpha} = \left(\frac{S_r s}{S_{r0} s_0}\right)^{\alpha} \quad (1)$$

The values of suction s and degree of saturation S_r of the blank test at a mean net stress $p'' = 0$ are given in Figure 7, and p'_0 represents the constitutive stress at the as-compacted conditions ($p'_0 = S_{r0} s_0 = 0.4$ MPa, according to Table 2). A value of $\alpha = 0.53$ was obtained by least squares minimisation, which is close to the usually suggested value $\alpha = 0.50$ (see, for instance, Suriol *et al*. 2014). The modelled curve is shown in Figure 8b. The same expression (1) was used to plot the evolution of G/G_0 of the treated sample, again inferring the suction and the degree of saturation values from the data in Figure 7, but a higher value of $\alpha = 0.90$ was obtained by fitting. Interestingly, the model correctly accounts for the reduction in G/G_0 between days 7 and 13, during which the sample undergoes a slight increase in S_r (from 70% to 72%) with suction decreasing from 1.5 MPa to 1.3 MPa.

The contribution of the bio-treatment to the small-strain shear stiffness is evaluated by calculating the difference ΔG between the value of G at given curing times and the initial value G_0, normalised with respect to G_0. The data of the samples cured in the 'open-system' were corrected for the effect of drying, by calculating the difference between the actual value and the corresponding blank value at the same suction and

degree of saturation (the retention data in Figure 2 showed no appreciable differences between untreated and treated samples). The results presented in Figure 9 measure the stiffening effect produced by the bio-treatment alone. This stiffness increase with the time of curing t for both the 'closed-system' and the corrected 'open-system' series can be fitted to the curve

$$\frac{\Delta G}{G_0} = \left(\frac{t + t_r}{t_r}\right)^{\beta} - 1 \qquad (2)$$

with a reference time t_r = 0.9 days and an exponent β = 0.20.

Concluding remarks

The bio-treatment presented by Morales *et al*. (2015), conceived to reduce costs and potential impact of produced ammonia to a minimum, was enhanced in this new test series, by slightly changing the compaction procedure. The samples with bacteria were cured after compaction, under two different evaporation boundary conditions. Mechanical improvement was tracked through the evolution of small-strain stiffness, measured by bender elements, and ancillary tests were performed to interpret and confirm the previous results. The test results revealed consistent increase in the small-strain shear stiffness during the ageing period due to the microbiological treatment, which could be appreciated following the 'closed-system' curing technique, and also on the 'open-system' cured samples after correcting the data for the suction increase due to evaporation. The results of this investigation show that even a *soft* biological treatment can provide some improvement to soils available on site, in order for them to become eligible for earth structures, provided appropriate protocols are followed during the construction. The actual improvement effects can be quantified in the laboratory by trying to replicate the possible field protocol.

Acknowledgements

The first author wishes to acknowledge the University of Almería for providing her research grant. Special thanks are due to the Department of Biology and Geology, in particular Dr. Joaquín Moreno and Juan Antonio López-González, for assisting in the microbiological analyses. The authors acknowledge the contribution of Dr. Jubert Pineda in the experimental setup and interpretation of the bender elements results.

References

Al Qabany A., Soga K. & Santamarina C. (2012). Factors affecting efficiency of microbially induced calcite precipitation. J. Geotech. Geoenviron. Eng. ASCE 138(8): 992-1001.

Arroyo M., Pineda J. & Romero E. (2010). Shear wave measurements using bender elements in argillaceous rocks. Geotechnical Testing Journal 33(6): 488-498.

ASTM 2010 Standards: Soil & Rock. V. 04.08. Philadelphia.

DeJong J.T., Soga K., Kavazanjian E., Burns S., van Paassen L., Fragaszy R., Al Qabany A, Aydilek A., Bang S.S., Burbank M., Caslake L., Chen C.Y., Cheng X., Chu J., Ciurli S., Fauriel S., Filet A.E., Hamdan N., Hata T., Inagaki Y., Jefferis S., Kuo M., Laloui L., Larrahondo J., Manning D., Martinez B., Mortensen B., Nelson D., Palomino A., Renforth P., Santamarina J.C., Seagren E.A., Tanyu B., Tsesarsky M. & Weaver T. (2013). Biogeochemical processes and geotechnical applications: Progress, opportunities, and challenges. Géotechnique 63(4): 287-301.

Hammes F. & Verstraete W. (2002). Key roles of pH and calcium metabolism in microbial carbonate precipitation. Re. Environ. Sci. Bio/Technol. 1: 3-7.

Morales L., Garzón E., Romero E. & Jommi C. (2010). Effects of a microbiological compound for the stabilisation of compacted soils on their microstructure and hydro-mechanical behaviour. Proc. 5th Int. Conf. Unsaturated Soils, Barcelona, September 6-8. Unsaturated Soils. E.E. Alonso & A. Gens (eds). Taylor & Francis Group, London 1: 573-578.

Morales L., Romero E., Pineda J.A., Garzón E. & Giménez A. (2012). Ageing effects on the stiffness behaviour of a microbiologically treated and compacted soil. Proc.2nd European Conf. Unsaturated Soils, Naples, June 20-22. Unsaturated

Soils: Research and Applications. C. Mancuso, C. Jommi & F. D'Onza (eds). Springer, Berlin 1: 371-376.

Morales L., Romero E., Jommi C., Garzón E. & Giménez A. (2015). Feasibility of a soft biological improvement of natural soils used in compacted linear earth construction. Acta Geotechnica 10: 157-171.

Pineda J.A. (2012). Swelling and degradation of argillaceous rocks induced by relative humidity effects: an experimental study. PhD Thesis, Universitat Politècnica de Catalunya, Barcelona.

Romero E. (2013). A microstructural insight into compacted clayey soils and their hydraulic properties. Engineering Geology 165: 3-19.

Romero E., Della Vecchia G. & Jommi C. (2011). An insight into the water retention properties of compacted clayey soils. Géotechnique 61(4): 313-328.

Stocks-Fischer S., Galinat J. K. & Bang S. S. (1999). Microbiological precipitation of $CaCO_3$. Soil Biol. Biochem. 31(11): 1563-1571.

Suriol J., Romero E., Lloret A. & Vaunat J. (2014). Small-strain shear stiffness of compacted clays: Initial state and microstructural features. Proc. 6th Int. Conf. on Unsaturated Soils, Sydney, July 2-4. Unsaturated Soils: Research & Applications. N. Khalili, A.R. Russell & A. Khoshghalb (eds.). Taylor & Francis Group, London 1: 769-775.

TABLES:

Table 1. Physical and chemical properties of untreated and treated samples.

Sample	Consistency limits		Particle size			Density solids	Specific surface	$CaCO_3$	Organic matter	Gypsum
	w_L (%)	*PI* (%)	<425µm (%)	<75µm (%)	<2 µm (%)	ρ_s (Mg/m^3)	S_s (m^2/g)	% dry mass	(%)	(%)
Untreated	48	30	70	50	23	2.73	33-46	1.1[a]-4.5[b]	0.39	0.91
Treated*	49	29	40[+]	2[+]	0[+]	2.74	32-44	1.8[a]-6.4[b]	0.16	0.12
Treated_NT	41	24	-	-	-	2.73	-	4.7[a]-8.8[b]	0.17	0.24

* Morales *et al*. (2015)

[+] With aggregations created on treatment

[a] Bernard

[b] Dietrich-Frühling

Table 2. Proctor compaction data of the untreated material. Initial state of the statically compacted soil matching standard Proctor at optimum conditions.

Standard Proctor (0.6 MJ/m^3)					Modified Proctor (2.7 MJ/m^3)		
ρ_d (Mg/m^3)	w (%)	S_r (%)	Suction,s (MPa)	Max. vertical stress* (MPa)	ρ_d (Mg/m^3)	w (%)	S_r (%)
1.85	15.0	87	0.5	1.0	2.05	11.4	94

* Equivalent static compaction stress to achieve the same dry density (at the same water content) of standard Proctor at optimum conditions

FIGURES:

Figure 1. Steps followed on soil samples preparation.

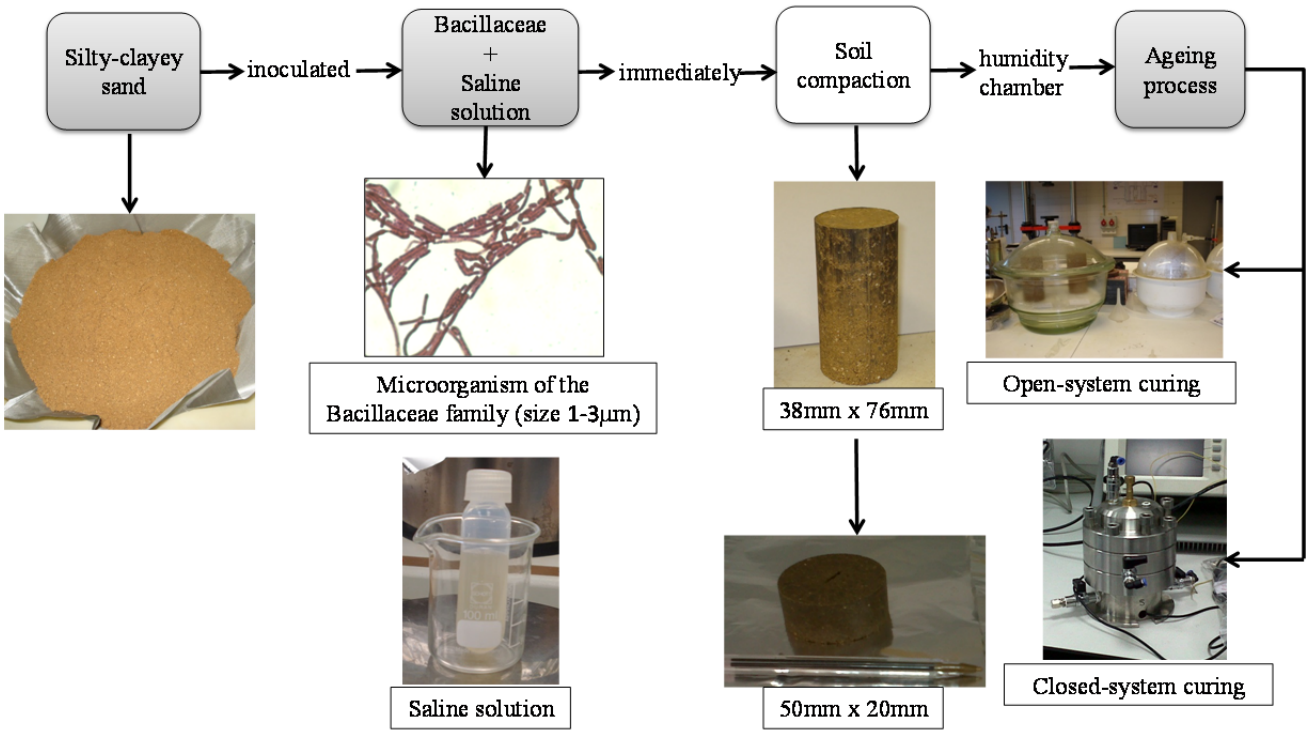

Figure 2. Water retention data upon drying for the new samples ('NT'), compared with data from Morales *et al*. (2015).

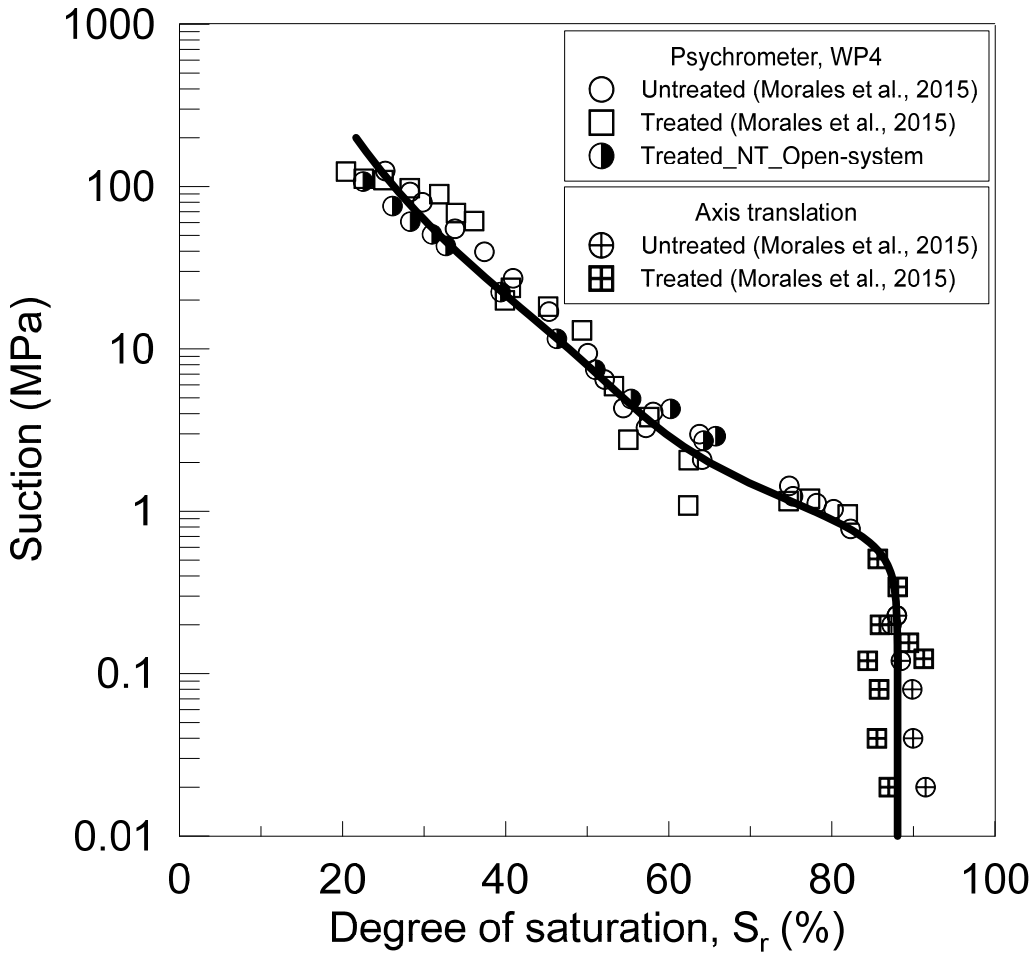

Figure 3. Cumulative distributions and pore size density functions for untreated and 'NT' samples derived from MIP data.

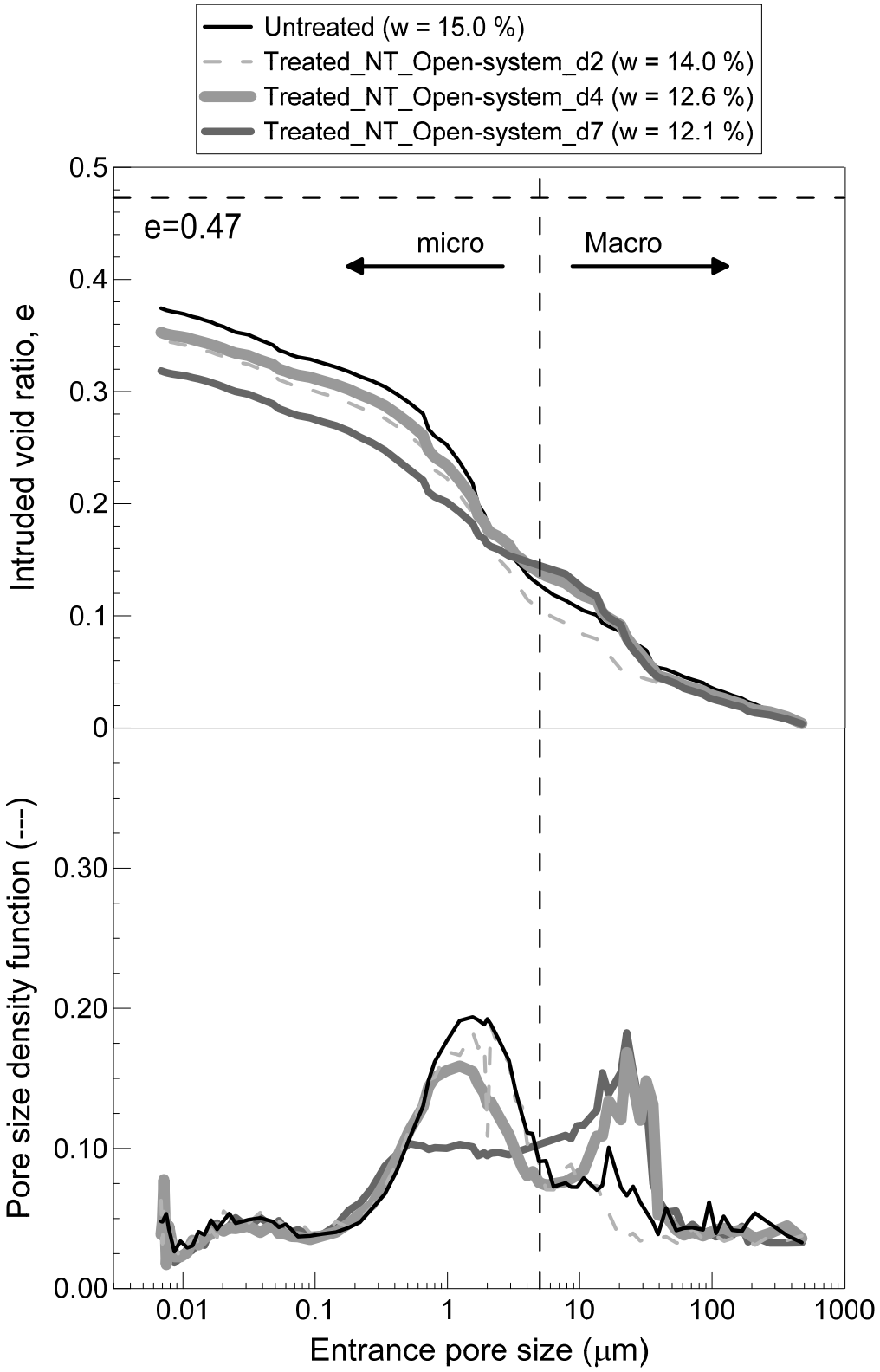

Figure 4. Micro- and macro-void ratio evolution during ageing for treated ‘NT’ samples cured under ‘open-system’ conditions.

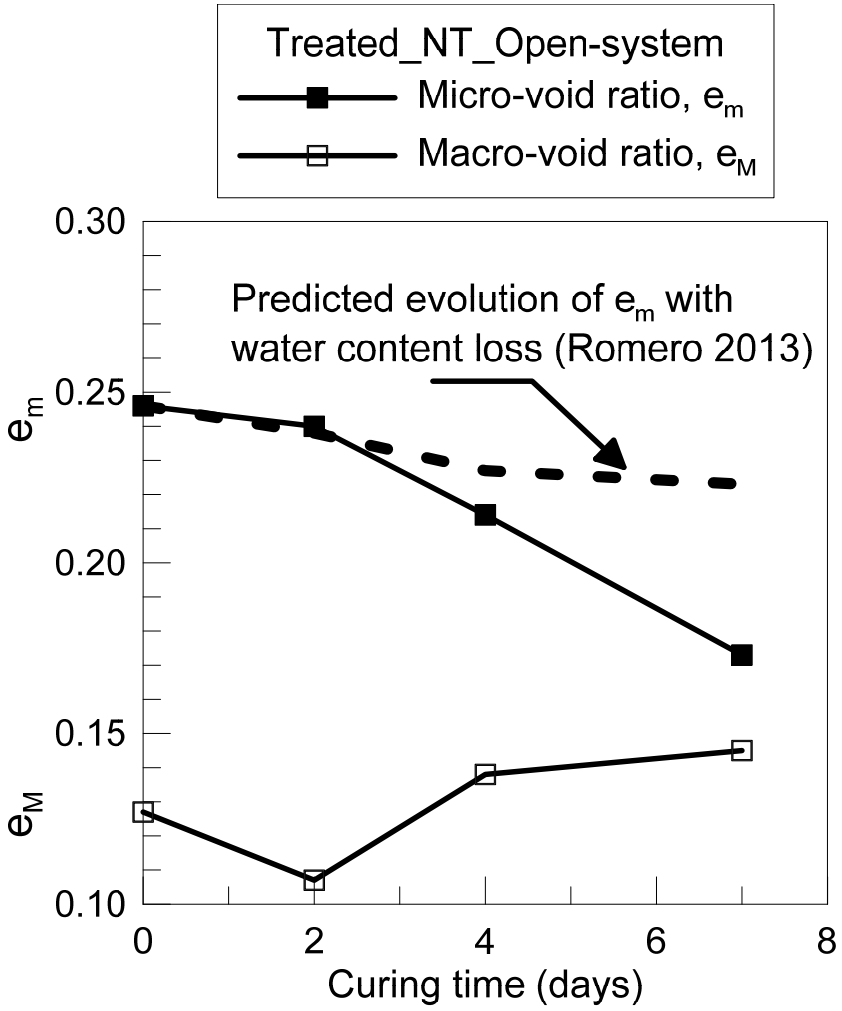

Figure 5. (a) Deviatoric stress-axial strain curves for treated ‘NT’ soils at different ageing periods. (b) Time evolution of peak unconfined compression strength and splitting tensile strength during the incubation process.

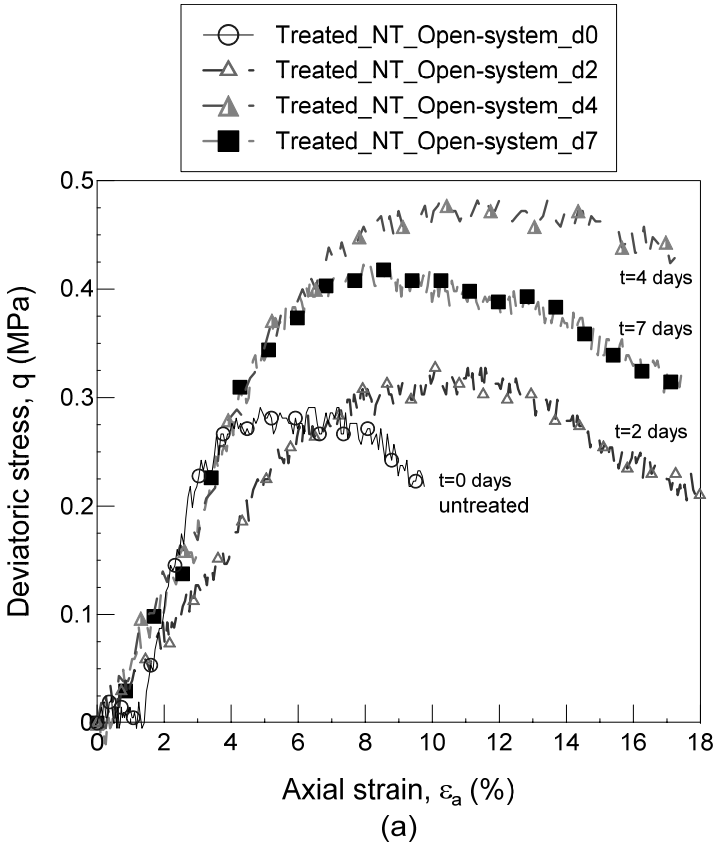

(a)

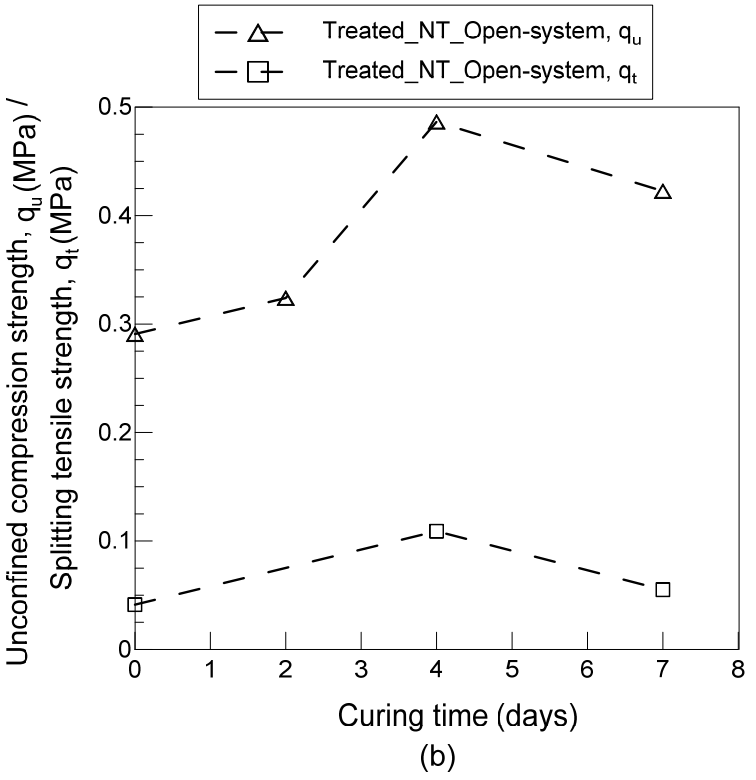

(b)

Figure 6. Evolution of small-strain shear moduli with ageing for the ‘open-system’ and ‘closed-system’ protocols. Initial and final degrees of saturation. Resonant column test on untreated sample (Morales *et al*. 2015).

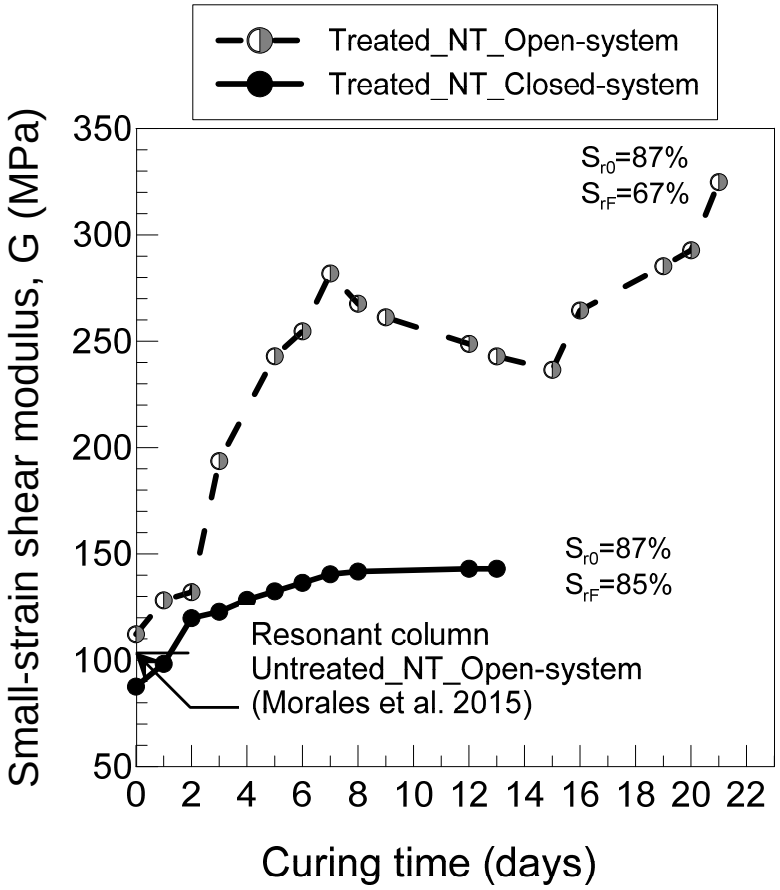

Figure 7. Degree of saturation and suction changes during ‘open-system’ curing. Blank test results following ‘open-system’ curing on untreated sample.

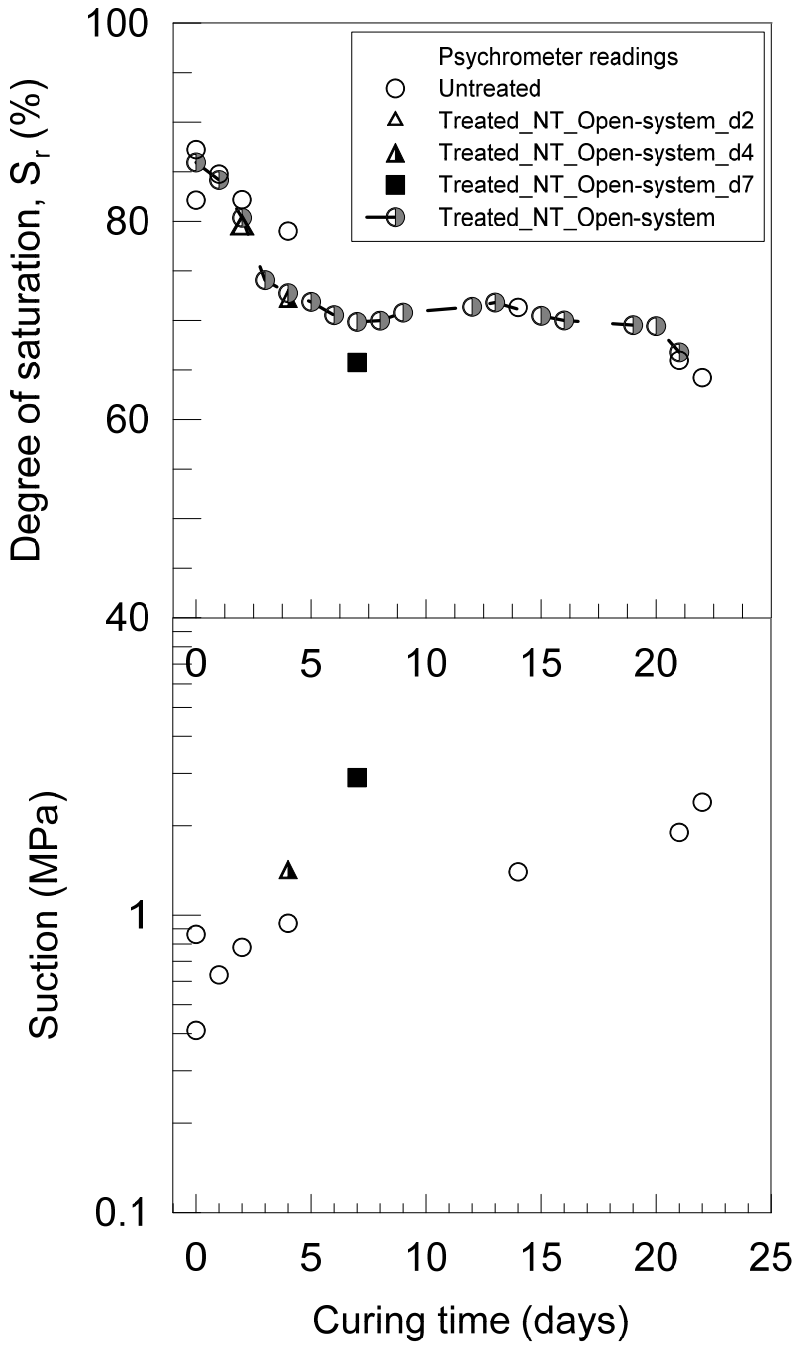

Figure 8. (a) Evolution of normalised values G/G_0 with degree of saturation for 'NT' and blank test samples following the 'open-system' curing protocol.(b) Time evolution of G/G_0 along 'open-system' curing ('NT' and blank test samples).

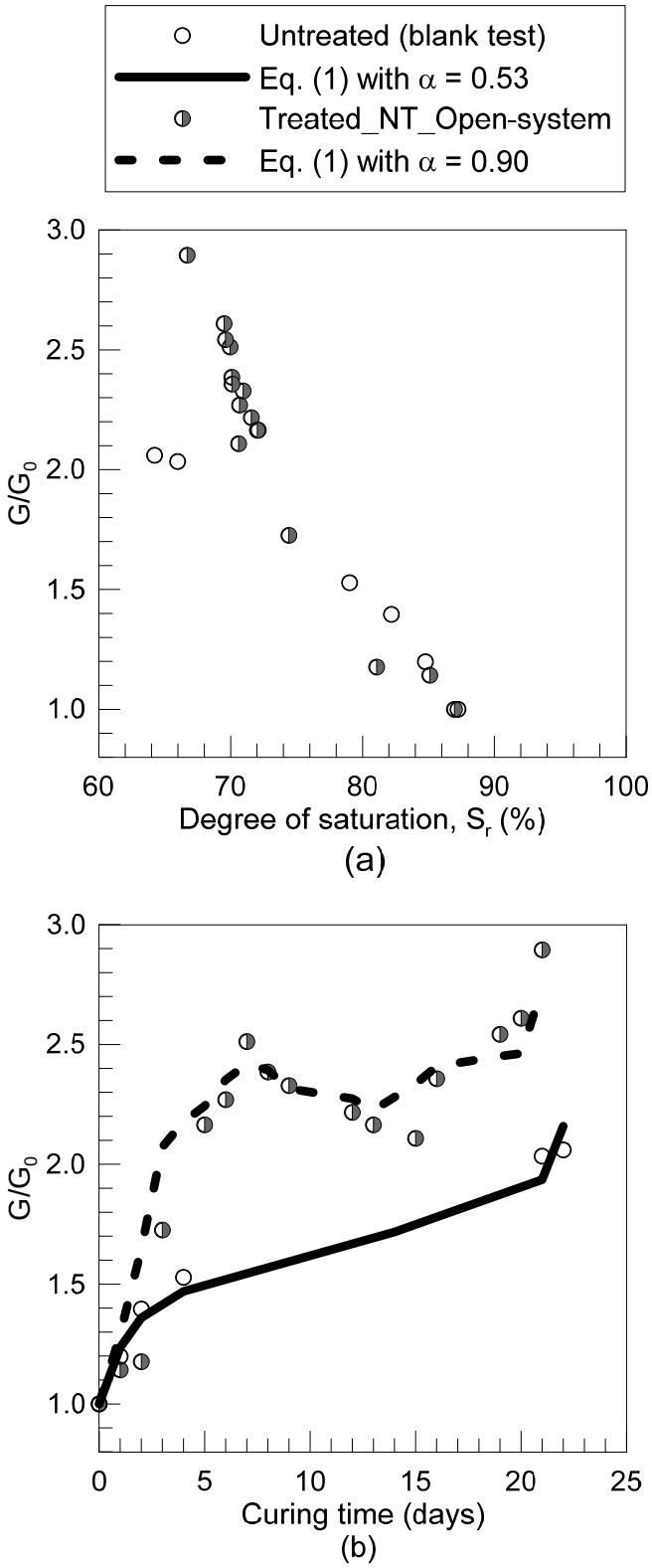

Figure 9. Variation of $\Delta G/G_0$ during 'open-system' and 'closed-system' curing. Corrected values for 'open-system' curing. Solid line: Eq.(2) with $t_r = 0.9$ days and $\beta = 0.20$.